TCAD-Optimization Coupling Enabled TID Modeling and Calibration of Commercial SiC Power MOSFET

Xujiao Gao
Electrical Models & Simulation, Sandia National Laboratories, Albuquerque, NM 87123
(505) 844-7179, Email: xngao@sandia.gov

Corresponding (and Presenting) Author:

Xujiao Gao, Sandia National Laboratories, Albuquerque, NM 87123

Contributing Authors:

Jaideep Ray, Elaine L. Rhoades, Josh M. Young, Brian D. Rummel, Larry Musson, Thomas E. Buchheit

Sandia National Laboratories, Albuquerque, NM 87123

Abstract – We propose a TCAD-optimization coupling approach that allows to determine major device parameters in COTS devices. The coupling together with surrogate model and Bayesian calibration enables accurate TID modeling and calibration of commercial SiC MOSFET.

Presentation Preference: Oral Presentation
Session Preference: Basic Mechanisms of Radiation Effects in Electronic Materials and Devices

Index Terms: COTS, SiC power MOSFET, TCAD, tool coupling, total ionizing dose (TID), threshold voltage shift, surrogate model, Bayesian calibration.

Sponsors:
Sandia National Laboratories is a multimission laboratory managed and operated by National Technology & Engineering Solutions of Sandia, LLC, a wholly owned subsidiary of Honeywell International, Inc., for the U.S. DOE's National Nuclear Security Administration under contract DE-NA-0003525. The views expressed in the article do not necessarily represent the views of the U.S. DOE or the United States Government.

I. INTRODUCTION

SILICON carbide (SiC) power MOSFETs have gained significant interest in power electronics, space and nuclear applications, due to their high breakdown voltage, high operating temperature, high frequency capability, and radiation tolerance [1-3]. There have been significant experimental works in the literature that study the total ionizing dose (TID) effects in these devices [4-6]. However, the physical processes of TID effects are known to be complicated, which involve hole trapping/de-trapping, possible electron trapping/de-trapping, annealing, and other processes [7-8]. Currently, there is no existing model that can capture these complex physical processes. In addition, in the case of SiC MOSFETs, Commercial-Off-The-Shelf (COTS) parts are often the only ones available for researchers to study their radiation properties. Given the nature of COTS parts, device details such as active region doping values are typically unknown or difficult to obtain, but they are essential to build a reliable TCAD device model.

To overcome the above-described obstacles in modeling radiation responses of COTS devices, we propose a TCAD-optimization tool coupling approach that allows us to determine key device details through parameter study and comparison with experimental data. After we obtained these key device parameters, we employed a Kimpton-like model [9] to simulate TID induced hole trapping process that captures the main feature of measured TID data. Then, based on TCAD simulations with varying parameters, we developed a surrogate model which enables Bayesian calibration to experimental data and consequently improves the prediction of simulations.

II. DAKOTA- CHARON TOOL COUPLING

Our proposed tool coupling approach combines the TCAD tool Charon [10] with Dakota [11], as shown in Fig. 1. Dakota is an open-source optimization and UQ tool that can be coupled to physics-based simulation tools such as Charon, Sandia's open-source TCAD code. This type of tool coupling offers two level of parallelization: (i) with Dakota as the outer driver, we can launch as many Charon simulations simultaneously as computing resource allows (e.g, N=2000 for one of our Dakota-Charon simulations); (ii) each Charon simulation runs in MPI parallel (e.g., a typical SiC Charon simulation runs on 384 processors in parallel).

The Dakota-Charon coupling allows us to perform a large number of simulations to determine important device dimensions and doping values. Additionally, this coupling allows us to conduct thousands of Charon simulations with varying key TID model parameters. These simulation results make it possible to develop a surrogate model and use it for Bayesian calibration to improve TCAD predictions.

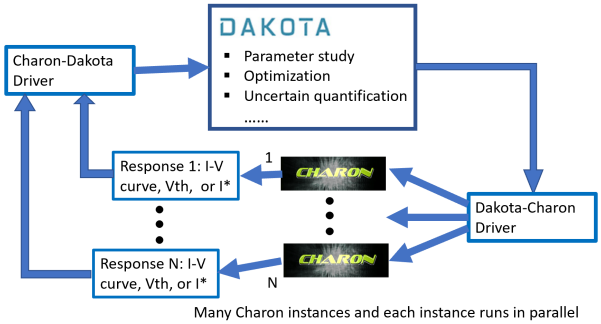

Fig. 1. Schematic of Charon and Dakota tool coupling.

III. DEVICE PARAMETERS ESTIMATION

We applied the Dakota-Charon coupling approach to estimate critical device parameters in a 3.3 kV SiC power MOSFET from GeneSiC Semiconductor Inc. [12]. The left panel of Fig. 2 shows a representative SEM cross-section image of the SiC device showing two p-well regions (white color) and a full JFET region in between. From the SEM images, we calculated device geometric dimensions and boundaries of doping regions and created a half-finger simulation structure (Fig. 2, right). We identified five necessary device parameters, as indicated in Fig. 2, that must be determined for reliable TCAD simulations: drift region doping and thickness, p-well doping, JFET region n-doping, and channel mobility. However, the critical doping values are difficult to discern for commercial devices using measurement techniques. For example, Secondary Ion Mass Spectroscopy (SIMS) cannot measure these doping values due to the small lateral dimension (a few μm) of a single-finger gate region compared to the 50-to-100-μm-wide probing window required by SIMS. Atom Probe Tomography (APT) can probe doping in a few-μm-wide window, but it cannot measure

doping values below $5x10^{18}$ cm^{-3} and is unable to differ nitrogen (used as n-type doping in SiC) atoms from silicon [13]. Scanning Microwave Impedance Microscopy (SMIM) may resolve dopant densities at the size scales of interest, but SMIM requires a high-quality calibration that is difficult to obtain for SiC material. In this study, the five key parameters are therefore determined using Dakota-Charon simulations based on device physics principles.

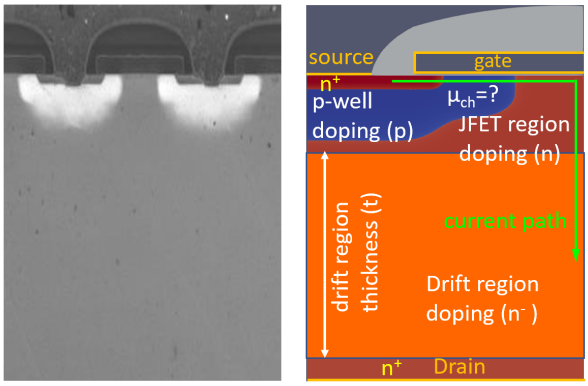

Fig. 2. Left: SEM cross-section image of a GeneSiC 3.3 kV SiC power MOSFET showing two p-well (white color) and a full JFET regions. Right: Charon simulation structure (half-finger) informed by SEM images showing the current path (green arrow) and five main device parameters that need to be determined from simulations. Source, drain, and gate contacts are also denoted.

Since the drift region thickness and doping determine the device breakdown voltage, we performed breakdown simulations using Charon across a wide parameter space of thickness and doping values. For the simulations, the gate and source contacts are grounded while the drain contact is swept with a positive bias, which reversely biases the p-well and n-drift junction. Figure 3 depicts simulated breakdown current-voltage curves showing the dependence of breakdown voltage on the drift region thickness and doping. We observe the simulated breakdown voltage for the dotted blue curve is about 3.8 kV, which gives a good margin compared to the 3.3 kV breakdown voltage given in the device datasheet. Hence, we chose the drift region thickness to be about 27 μm and the doping to be around $3x10^{15}$ cm^{-3}.

To estimate the p-well doping, we ran drain current (I_{DS}) vs. gate voltage (V_{GS}) Charon simulations for a range of doping values. Some of the results are plotted in Fig. 4. Clearly, p-well doping has a dominant effect on the threshold voltage. We observe that a doping of $1.4x10^{17}$ cm^{-3} produces current and voltage values that show good

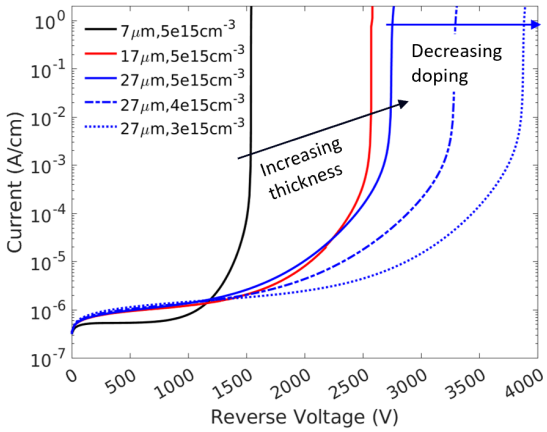

Fig. 3. Simulated breakdown current-voltage curves (selected for plot clarity) showing the dependence of breakdown voltage on the drift region thickness and doping.

agreement with measured data around the threshold as indicated by the green circle. Hence, we chose the p-well doping to be $1.4x10^{17}$ cm^{-3} with a Gaussian decay width of about 0.5 μm in our simulations.

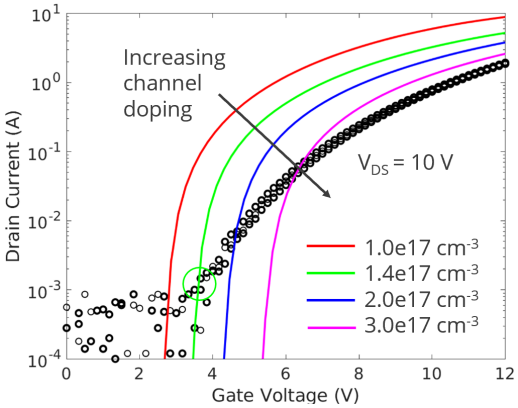

Fig. 4. Simulated drain current vs. gate voltage curves showing the dependence of threshold voltage and current with p-channel doping. Black circles are experimental data for three device samples.

It is a well-known design rule to use a higher n-doping in the JFET region than the drift region for current spreading and low resistance in power MOSFETs [14]. Therefore, to estimate the JFET n-doping, we ran Charon simulations for a range of values starting from $3x10^{15}$ cm^{-3} and examined how the current path between source and drain regions changes with doping. We observed that when the JFET n-doping is below $3x10^{16}$ cm^{-3}, the JFET n-region is fully or nearly depleted of electrons when a typical drain voltage (e.g., V_{DS} = 10 V) is applied, which inhibits current conduction or makes it difficult to form a current path. Hence, a JFET n-doping of $3x10^{16}$ cm^{-3} was selected to maintain a robust current path in the forward operating regime.

The last important parameter to estimate is the channel mobility. We first employed Dakota-Charon simulations to find the channel mobility values as a function of gate voltages such that simulated I_{DS}-V_{GS} curves match with measured data. From this, we proposed an exponentially field dependent channel mobility model as:

$$\mu_{ch} = \mu_1 exp\left(\frac{|F|}{F_1}\right) + \mu_2 ex\,p\left(\frac{|F|}{F_2}\right).$$

The first exponential term intends to dominate the I_{DS}-V_{GS} curve at low voltages, while the second one has a stronger effect at high gate voltages. Parameters, i.e., (μ_1, F_1, μ_2, F_2) in the model were optimized through Dakota-Charon simulations. Their values were chosen when simulated curves match with measured data. Simulation results using the informed device parameters show a good agreement with measured data in a non-radiation environment as shown in Fig. 5.

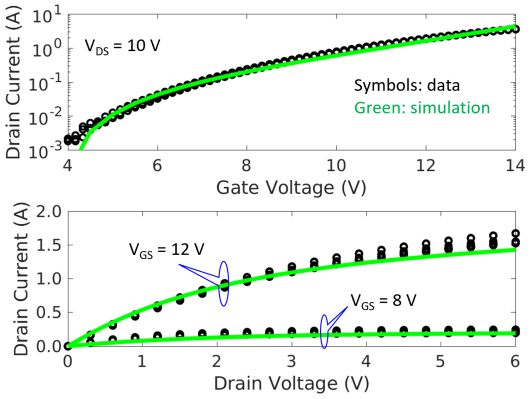

Fig. 5. Simulated current-voltage curves (top: I_{DS}-V_{GS} curves with V_{DS} = 10 V. bottom: I_{DS}-V_{DS} curves) in comparison with measured data (black symbols).

IV. TID Modeling and Calibration

To study the TID response of the 3.3 kV SiC power MOSFET, extensive experiments have been conducted at the ACRR, IBL, and LINAC facilities [15]. We observed that TID radiation causes a negative shift in the threshold voltage (V_{th}) of the device and the voltage shift is saturated at high TID doses as shown in Fig. 6. It is widely accepted that the negative voltage shift is due to TID induced holes trapped near the SiO_2/SiC interface under the gate region [7-8]. Though electron traps could be formed at an interface and cause positive V_{th} shift, the formation of electron traps occurs on a much longer time scale than hole traps and they do not anneal after radiation [7-8]. Therefore, we believe hole traps at the SiO_2/SiC interface are mainly responsible for the observed V_{th} shift in the device under study.

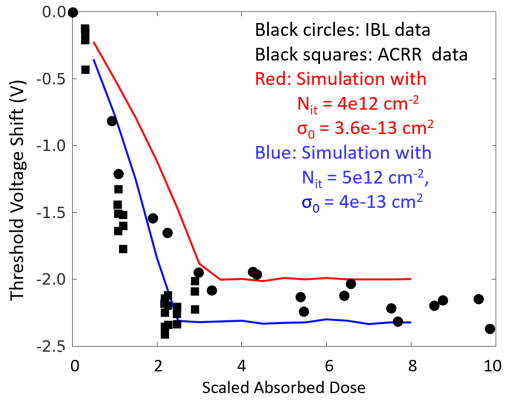

Fig. 6. Simulated V_{th} shifts (solid lines) with scaled absorbed doses in comparison with measured data (symbols).

TID induced negative V_{th} shifts are often modeled by adding fixed positive charges at the interface under the gate, which, however, cannot capture the saturation of V_{th} shifts at high doses. Therefore, we utilize the Kimpton TID model [9] which simulates field-dependent hole trapping and de-trapping processes. Analysis of the model reveals that when the rate of hole trapping is equal to the de-trapping rate, the net trapped hole charges are saturated at high doses and lead to the saturation of V_{th} shift. By enforcing the saturation of net trapped holes in Charon and by choosing proper interface trap density (N_{it}) and hole capture cross section (σ_0) at 1 MV/cm, we can simulate the saturation of V_{th} shifts at high doses as shown in Fig. 6.

The next question is what other N_{it} and σ_0 values would provide good calibration between simulation and experiment. To address this, we ran many Dakota-Charon simulations for different TID, N_{it} and σ_0 values. Based on these results, we selected the top 25% of them that are close to the experimental data as training data to develop a surrogate model using random forests [16], i.e., $\Delta V_{th}^{SM} = f_{RF}(TID, N_{it}, \sigma_0)$, which has $R^2 = 0.99$, indicating a good fit to Charon results. Based on the surrogate model, we performed Bayesian calibration [17] to the IBL data and obtained the posterior probability distribution function (PDF) of N_{it} and σ_0 as shown in Fig. 7. The sharp PDF of N_{it} indicates this parameter is easy to estimate, while the broad and flat PDF of σ_0 suggests it is difficult to estimate, which implies the uncertainty associated with σ_0 estimate is large.

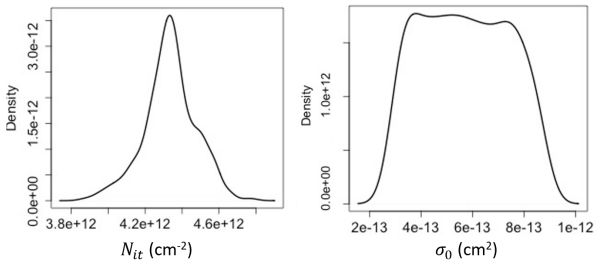

Fig. 7. Posterior PDF of N_{it} (left) and σ_0 (right) obtained from Bayesian calibration to the IBL data. The y-axis values are chosen such that the integration of PDF is 1.

From the posterior PDF of parameters, we randomly generate parameter samples and use them in Charon simulations. As an example, we generated 100 sampling points in the (N_{it}, σ_0) parameter space at 9 TID doses and ran 900 Charon simulations using these samples. The resulting average V_{th} shifts for these simulations are plotted as the blue curve in Fig. 8. Clearly, Charon results using parameters from the posterior PDF predict the IBL data very well. Similar Bayesian calibration work has been done for ACRR and LINAC data and will be discussed at the conference.

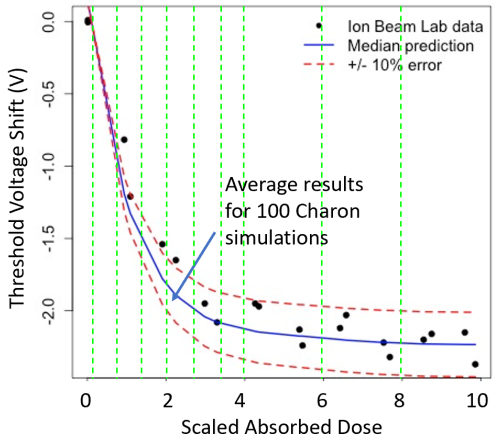

Fig. 8. Average Vth shifts (blue curve) computed from 100 Charon simulations as a function of scaled doses together with the IBL data (black circles). Red dashed lines indicate +/- 10% error from the blue curve, and the vertical green dashed lines denote positions of the 9 TID doses considered.

V. Conclusion

We have presented the TCAD-optimization (Charon-Dakota) tool coupling approach that allows us to determine major device parameters for a commercial 3.3 kV SiC MOSFET. Simulation results using informed device parameters show a good agreement with measured pre-radiation data. We have also achieved accurate calibration of TID induced V_{th} shifts between simulation and experiment utilizing the tool coupling together with surrogate model and Bayesian calibration. We plan to include and calibrate fractional hole yield in the TID modeling parameter space to inform the yield for a radiation facility. The presented simulation approach is also applicable to simulate other COTS parts. The resulting surrogate model can be used to either inform a TID-aware compact model development or directly as a compact model.

References

[1] A. Bolotnikov *et al*., "3.3kV SiC MOSFETs designed for low on-resistance and fast switching," *24th International Symposium on Power Semiconductor Devices and ICs*, Bruges, Belgium, 2012, pp. 389-392.

[2] X. Huang *et al.*, "Design and fabrication of 3.3kV SiC MOSFETs for industrial applications," *29th International Symposium on Power Semiconductor Devices and IC's (ISPSD)*, Sapporo, Japan, 2017, pp. 255-258.

[3] J. -M. Lauenstein *et al.*, "Space radiation effects on SiC power device reliability," *2021 IEEE International Reliability Physics Symposium (IRPS)*, Monterey, CA, USA, 2021, pp. 1-8.

[4] K. Gao *et al.*, "Degradation behavior and mechanism of SiC power MOSFETs by total ionizing dose irradiation under different gate voltages," *2021 IEEE Workshop on Wide Bandgap Power Devices and Applications in Asia (WiPDA Asia)*, Wuhan, China, 2021, pp. 46-50.

[5] Y. Sun *et al.*, "Investigation of total ionizing dose effects in 4H–SiC power MOSFET under gamma ray radiation," *Radiation Physics and Chemistry*, vol. 197, art. 110219, pp. 1-6, 2022.

[6] Q. Yu *et al*., "Application of total ionizing dose radiation test standards to SiC MOSFETs," in *IEEE Transactions on Nuclear Science*, vol. 69, no. 5, pp. 1127-1133, May 2022.

[7] T. R. Oldham and F. B. McLean, "Total ionizing dose effects in MOS oxides and devices," *in IEEE Transactions on Nuclear Science,* vol. 50, no. 3, pp. 483-499, June 2003.

[8] J. R. Schwank *et al*., "Radiation Effects in MOS Oxides," in *IEEE Transactions on Nuclear Science*, vol. 55, no. 4, pp. 1833-1853, Aug. 2008.

[9] Derek Kimpton and John Kerr, "A simple trap-detrap model for accurate prediction of radiation induced threshold voltage shifts in radiation tolerant oxides for all static or time variant oxide fields," *Solid-State Electronics*, vol. 37, no.1, pp. 153-158, 1994.

[10] https://charon.sandia.gov.

[11] https://dakota.sandia.gov/.

[12] https://genesicsemi.com/sic-mosfet/G2R1000MT33J/.

[13] Private communication with an APT expert from the EAG Labs (https://www.eag.com/), November 2023.

[14] T. Kimoto and J. A. Cooper, "Fundamentals of Silicon Carbide Technology," John Wiley & Sons, 2014, pp. 312-325.

[15] D. R. Hughart *et al.*, "Radiation response and initial facility comparison for 3.3 kV SiC power MOSFETs," Sandia Report, SAND2023-00940, September 2022.

[16] T. Hastie *et al.*, "The Elements of Statistical Learning," Springer, 2nd edition, 2009. Chapter 15, "Random Forests", pp. 587-604.

[17] R. Smith, "Uncertainty Quantification -Theory, Implementation and Applications," 1st edition, 2014, pp. 155-186.

VI. Acknowledgements

We would like to thank D. R. Hughart, J. E. Manuel, M. L. Breeding, and C. E. Glaser for their support in collecting experimental data. We would also like to thank A. Binder, L. Yates, B. Kaplar, and K. A. Maupin for many helpful discussions.